A New Explanation for the Origin of Superconductivity Based on Electron Magnetic Chains with 8-Shaped Magnetic Moments

Author: Sun Zhao
Affiliation: Shenzhen Relativity Technology Co., Ltd., Shenzhen, Guangdong 518000
Contact Email: e.mcc@163.com

Abstract

Since the discovery of superconductivity in 1911, its microscopic mechanism has remained a central challenge in condensed matter physics. The classical BCS theory, which uses lattice phonons as mediators to establish a Cooper pair model of two electrons, can explain the basic properties of low-temperature metallic superconductivity but faces several inherent limitations: phonon coupling is only a short-range interaction, unable to resolve the cross-scale contradiction of long-range synchronous coupling among a large number of electrons, and struggles to counteract the Coulomb repulsion between electrons. This theory fails to explain experimental phenomena such as pre-paired pseudogaps and non-monotonic changes in critical temperature under magnetic fields, while also being incompatible with novel systems like high-temperature and two-dimensional flat-band superconductivity.

This paper cites the **8-shaped electromagnetic standing wave + intrinsic drift electron structure** model [1], proposing the **electron magnetic chain** microscopic conductive structure: under an external field, the intrinsic drift within electrons is suppressed, causing their inherent **8-shaped magnetic moment** and magnetic coupling effects to manifest. Through the continuous chain-like connection enabled by the **8-shaped magnetic moment** attraction, without fixed limitations on the number of paired electrons, a long-range ordered arrangement forms conductive pathways. This model can uniformly cover conventional and high-temperature superconducting phenomena, systematically resolving all existing internal contradictions in BCS theory, and provides a quantifiable theoretical basis for the structural design of new high-temperature and even room-temperature superconducting materials.

Keywords

Superconductivity; 8-shaped magnetic moment electron magnetic chain; BCS Cooper pairs; electron intrinsic drift; origin of Cooper pairs; dense electron array

1.0 Introduction

The microscopic formation mechanism of Cooper pairs is a core fundamental issue in the field of superconductivity. The BCS theory established in 1957[2], relying on electron-phonon coupling, successfully explains the pairing behavior of conventional low-temperature superconductors. However, with experimental discoveries such as high-temperature superconductivity[3], pressure-regulated superconductivity, and reentrant superconductivity,

this theory exhibits multiple incoherent explanatory gaps regarding phenomena related to the evolution of Cooper pairs, urgently requiring supplementation of pairing mechanisms from the intrinsic electronic microstructure.

Common deficiencies in existing alternative theories

Phenomenological theories such as spin fluctuations, RVB, and multi-band can only adapt to single superconducting systems, lacking support from underlying electronic microstructures, and fail to uniformly describe the Cooper pair formation processes in both conventional and unconventional systems.

Research approach and scope of this paper

This paper does not negate the role of phonon coupling in conventional low-temperature superconductivity. Based solely on the topological structure of the electron**8-shaped magnetic moment**, we propose the inherent magnetic dipole interaction of electrons as a new binding channel, supplementing the formation pathway of ordered magnetic chain arrays in electrons, specifically addressing multiple experimental anomalies that the BCS theory struggles to interpret in detail.

Starting from the fundamental electromagnetic equations and the standing wave conditions, this paper forwardly deduces the formation conditions of electron ordering into chains under magnetic coupling and the variation laws of critical temperature, while providing observable experimental predictions. The entire text focuses solely on the microscopic physical image of electron magnetic chain formation through magnetic moment coupling, without attempting to provide a comprehensive interpretation of all macroscopic superconducting phenomena.

This study belongs to fundamental mechanism exploration, following the research paradigm of the classic BCS theory. It constructs a physical model based on publicly available experimental conclusions and fundamental electromagnetic laws, relying on logical self-consistency and observable predictions to support its research value. Compared to BCS's modeling approach of reverse-fitting parameters from experimental data, this paper starts from the microscopic topological structure of electrons, deduces the competitive relationship between electrostatic repulsion and magnetic moment attraction among electrons, refines the microscopic physical image of ordered chain-like electron arrangement, and fills the explanatory gaps in the traditional phonon pairing theoretical framework.

2.0 The Electron's Figure-8 Standing Wave Model

2.1 Introduction to the Electron's Figure-8 Standing Wave Model

The literature cited in this paper [1] proposes: **the "8-shaped electromagnetic standing wave + eigen drift electron structure"** model, which extracts only the core features directly related to Cooper pair formation. This model abandons the point-particle assumption of electrons, describing them instead as a self-consistent closed electromagnetic standing wave topological structure. The persistent 8-shaped standing wave circulation within the standing wave is the origin of the electron's spin property. The entire standing wave field extends outward, forming a bidirectional magnetic axis that penetrates the entire electron, endowing it with an intrinsic magnetic dipole characteristic. This chapter only lays the foundation for this microscopic electron structure; the role of magnetic axis coupling in Cooper pair formation will be derived in subsequent sections.

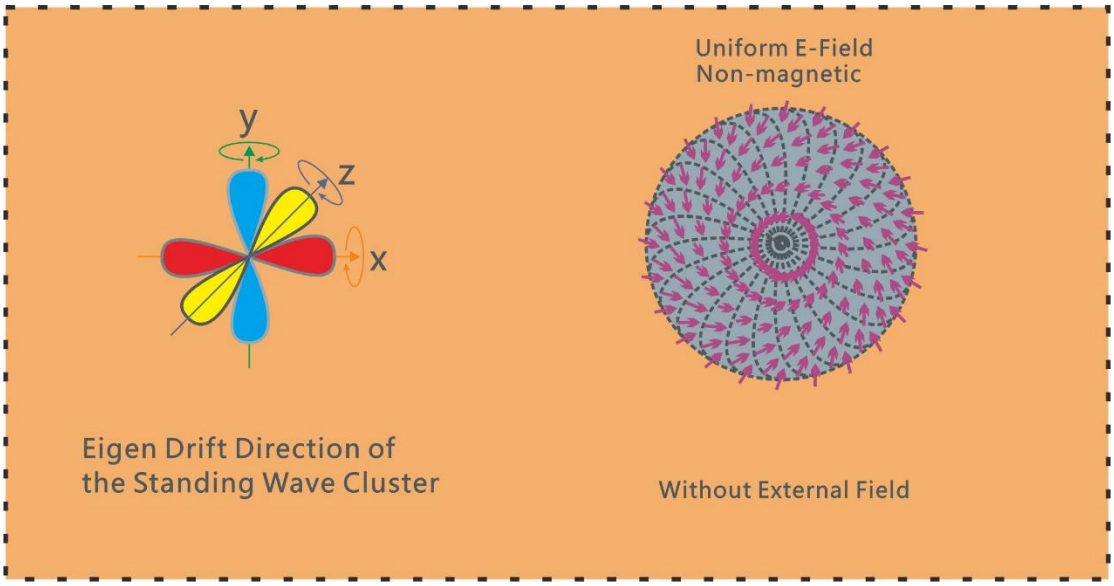

Figure 1 Eigen drift structure of the 8-shaped electromagnetic standing wave and its field distribution in zero external field

2.2 Formation Mechanism of the 8-Shaped Magnetic Moment Model

In the absence of an external field and under ambient conditions, the single-cluster figure-8 electromagnetic standing wave generates a natural centripetal force through its intrinsic interaction with the equivalent medium, maintaining a spherically symmetric steady-state topological structure. Within the unit, a pair of reverse magnetic axes coexist, their torques canceling each other, leaving the magnetic axes in a state of intrinsic drift-free equilibrium, with no directional deformation overall and no net macroscopic magnetic response.

When a uniform external magnetic field B is applied, the magnetic axes within the standing wave couple with the external field through magnetic moment interactions. The originally spherically symmetric figure-8 standing wave structure undergoes directional stretching, entering a state of intrinsic drift collapse: the standing wave is compressed perpendicular to the magnetic field direction and elongated along the field direction, transforming the spherical contour into an elongated non-circular boundary. The internal circulation streamlines of the standing wave are constrained and gathered by the magnetic field, causing the originally dispersed bidirectional magnetic axes to align orderly along the external field direction, with the equivalent negative charge of electrons uniformly distributed on the deformed outer contour.

To simplify the analysis of the complex microscopic circulation, this paper establishes a two-layer visual description: the left side shows a detailed schematic, fully retaining the figure-8 standing wave circulation streamlines, native standing wave magnetic axes, and the complete deformed topology; the right side presents an engineering-simplified equivalent model, omitting the dense internal streamlines and retaining only the deformed contour, paired magnetic axes, and boundary negative charge markers, visually illustrating the structural collapse induced by the external magnetic field.

The core value of this equivalent model lies in: simplifying the response of complex fluctuating topological external fields into a geometrically intuitive structure that can be directly deduced, clearly explaining the morphological changes of single electrons under external magnetic fields, while providing a standardized foundational unit for subsequent derivations of multi-electron coupling and ordered Cooper pair arrays. The deformation process is solely regulated by the

internal forces between the field and the medium. Lorentz-like constraint forces are always perpendicular to the intrinsic drift motion direction, consuming no inherent energy of the standing wave throughout the process. A steady-state distributed electric field does not generate electromagnetic radiation, and structural deformation belongs to steady-state reversible changes.

To facilitate a unified description throughout the text, this paper proposes: electrons naturally possess an 8-shaped closed standing wave topological structure, whose circulating current intrinsically carries a magnetic dipole. In the absence of an external field, the magnetic dipole orientations are random, exhibiting no net macroscopic magnetic response. Under an applied parallel magnetic field, the magnetic dipoles align directionally, allowing stable observation of collective magnetic coupling behaviors. This also precisely aligns with the principle of magnetic dipole potential energy balance in external fields, where the magnetic moment being parallel or antiparallel to the external field corresponds to the system's potential energy extremum states. This paper formally names the topological origin of this magnetic dipole as the **8-shaped standing wave topological magnetic dipole**, hereafter uniformly abbreviated as the **8-shaped magnetic moment**, also distinguishing it from Cooper pairs.

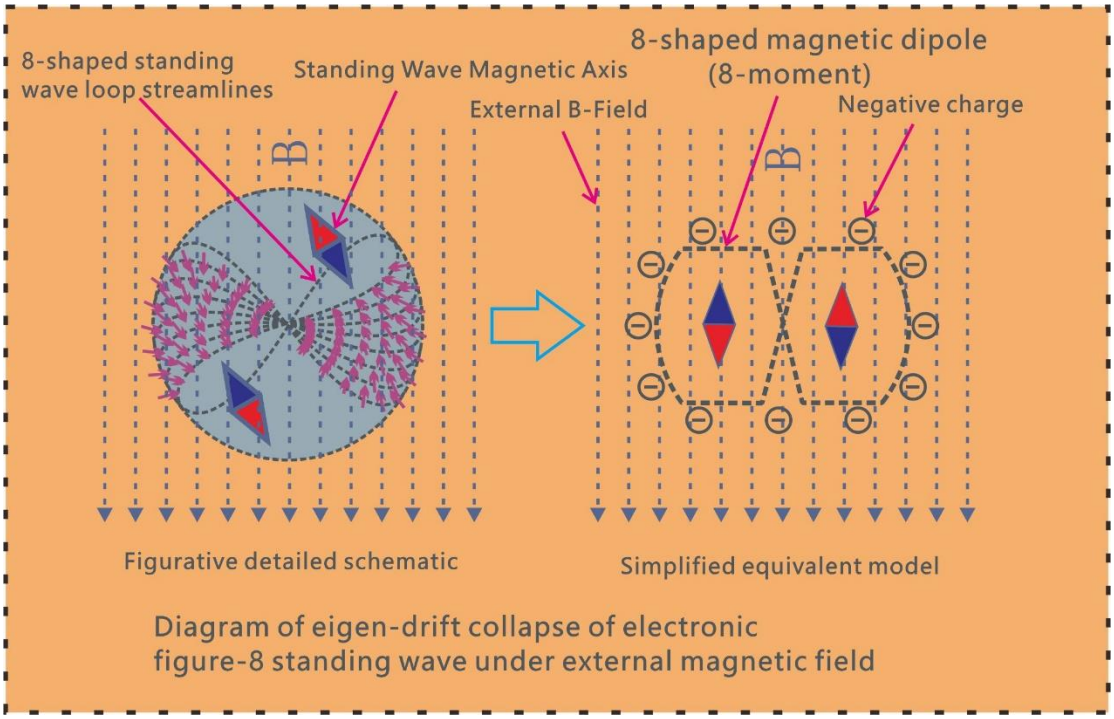

Figure 2 Schematic of eigen-drift collapse for electronic figure-8 standing wave under an external magnetic field

2.3 Coupling Mechanism of Multiple 8-shaped Magnetic Moments

Electron Magnetic Chain:

Based on the previously established **8-shaped magnetic moment** model under an external field, each equivalent **8-shaped magnetic moment** contour contains a pair of oppositely oriented magnetic dipoles. One magnetic moment aligns with the external magnetic field$B$, while the other is arranged opposite to it. The edges of adjacent electronic units are mutually fitted, and neighboring **8-shaped magnetic moments** generate complementary magnetic attraction effects through opposite magnetic axes, counteracting the original electrostatic Coulomb repulsion

between electrons to form a Cooper pair-like structured **electron magnetic chain**.

Forced Cooper Pair Pairing Mechanism:

The physical scenario of Cooper pairs[[TAG_27]] relying on phonons for pairing appears weak and contrived, with feeble and delayed gravitational effects, lacking a stable spatial confinement structure, and offering a pale explanatory logic for pairing.

In the diagram, adjacent eight-shaped magnetic moments are coupled with opposite magnetic poles to form a set of magnetic dipole pairs. Multiple eight-shaped magnetic moments are sequentially connected in series through opposite magnetic pole coupling to form the **electronic magnetic chain** . This is the most critical feature distinguishing it from Cooper pairs, as Cooper pairs are limited to the coupling between two electrons, whereas the formation of electronic magnetic chains here is not restricted by the number of electrons.

Instantaneous dissociation between electronic magnetic chains :

Since the magnetic polarity at both ends of the **eight-shaped magnetic moment** is formed by the internal eight-shaped electromagnetic standing wave circulation, the magnetic polarity on both sides changes with the frequency of the electromagnetic standing wave $f = \frac{c}{2R}$, R being the electron radius. Due to its extremely small value, the vibration frequency of the standing wave is very high. Therefore, whenever the internal standing wave of the **eight-shaped magnetic moment** crosses the zero point, the adjacent two **eight-shaped magnetic moments** instantaneously lose their magnetism, leading to transient chain breakage or so-called **instantaneous dissociation between electronic magnetic chains** .

Prerequisites for the formation of electronic magnetic chains:

Ultra-low temperature: Random thermal collisions of electrons continuously disturb the intrinsic drift of the internal 8-shaped standing wave, distorting the orientation of magnetic moments, widening the dissociation interval of magnetic coupling, and disrupting the heteropolar pairing structure. In extremely low-temperature environments, the thermal motion of electrons is significantly attenuated, and collision disturbances nearly vanish, **8-shaped magnetic moment** trajectories remain regular and stable. Low temperature provides a foundational environment for long-term magnetic dipole coupling, relying on the attractive force of heteropolar magnetic dipoles to counteract the electrostatic repulsion between electrons. A large number of electrons are orderly connected to form a continuous magnetic chain system with globally phase-locked coherence, establishing complete microscopic structural support for macroscopic superconducting effects such as zero resistance and the Meissner perfect diamagnetism.

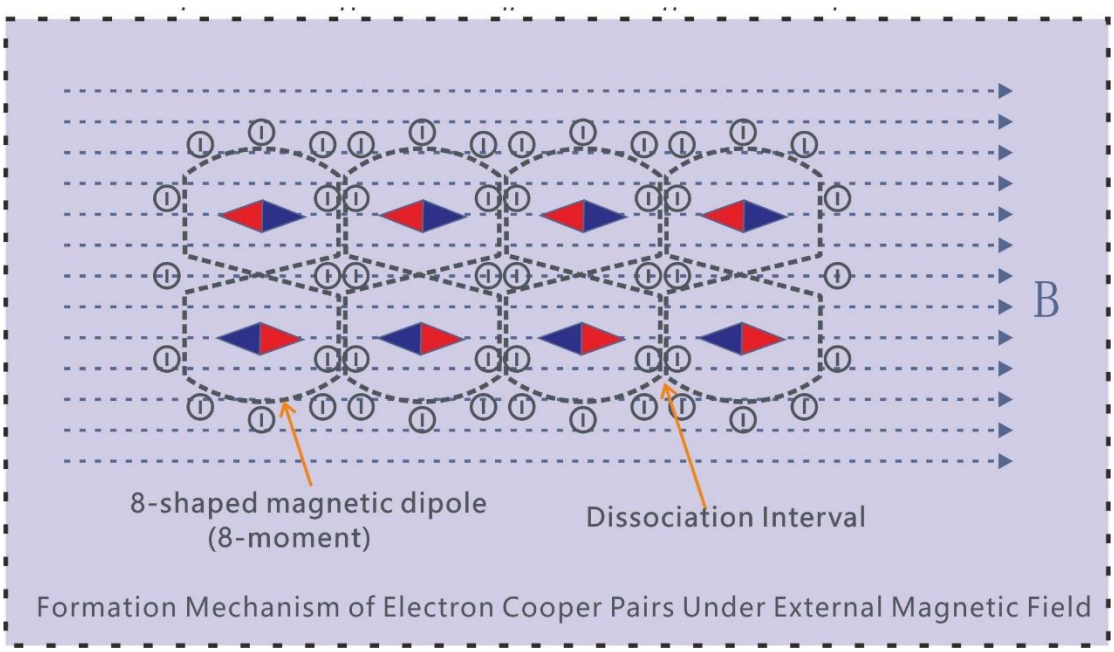

Figure 3 Formation mechanism of electron magnetic chains under external magnetic field

External field induction: A weak external magnetic field can impose directional constraints on the drift trajectories of the internal 8-shaped standing waves of electrons, unifying the arrangement orientation of all electron magnetic dipoles. This causes adjacent electrons **8-shaped magnetic moments** to automatically form heteropolar close-contact pairing, effectively suppressing the Coulomb electrostatic repulsion between electrons and laying an ordered foundation for the construction of long-range coherent electron magnetic chains. Without the directional effect of an external field, the magnetic moments of electrons are randomly and disorderly arranged, significantly reducing the probability of heteropolar coupling and making it difficult to form a globally coherent magnetic chain structure.

Current-induced magnetic field effect: The directionally transported charge carriers in a conductor generate a closed-loop self-induced magnetic field in the cross-section perpendicular to the current. At any point in the conductor, the direction of this self-field aligns with the tangential direction of the circular magnetic dipole attraction at that point, acting parallel to nearby electrons and inducing the formation of figure-8 magnetic moments. Thus, directional alignment of **figure-8 magnetic moments** can be achieved without an external magnetic field.

The self-induced magnetic field simultaneously constrains the alignment orientation of all figure-8 magnetic moments along the conductor, driving adjacent units to couple complementarily with opposite poles. These units interconnect within the cross-section perpendicular to the current, forming a closed-loop electron magnetic chain. This microscopic mechanism explains the intrinsic reason why a current-carrying superconducting loop can maintain a zero-resistance superconducting state without an external field, serving as the core condition for carrier self-driven pairing.

This self-field coupling effect causes current stratification in superconducting conductors, distinct from the skin effect in conventional conductors caused by alternating vortex fields, as their physical mechanisms are entirely different.

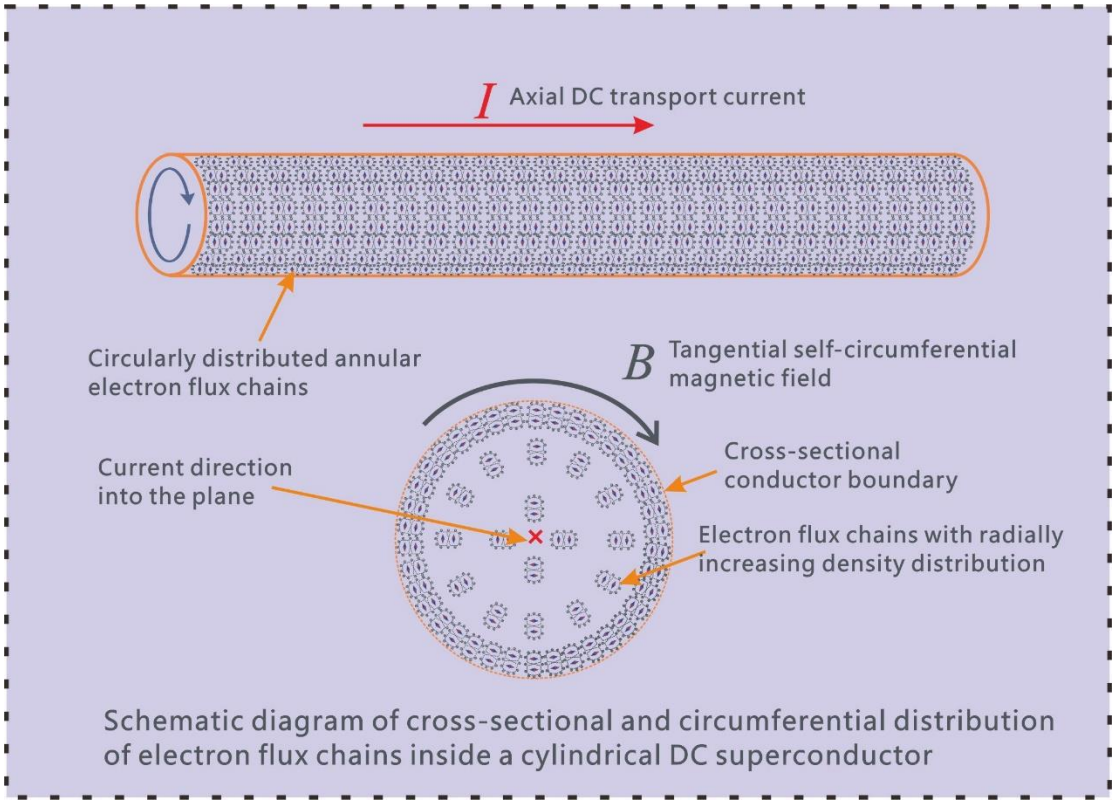

Figure 4 Schematic diagram showing the cross-sectional and circumferential distribution of electron magnetic chains within a cylindrical DC superconductor

---

3.0 Derivation of Electron Magnetic Chain Dynamics — 8-Character Magnetic Moment Pairing Evolution Mechanism

This chapter, based on the single-cluster **8-character magnetic moment** standing wave structure model, rigorously derives the energy criterion for the spontaneous formation of **electron magnetic chains** through the competition between electrostatic repulsion and alternating magnetic dipole attraction potentials among **8-character magnetic moments**, as well as the zero-coupling modulation effect of intrinsic drift **8-character magnetic moment** flipping. A microscopic pairing dynamics mechanism is established to explain low-temperature superconductivity ordering, zero resistance, perfect diamagnetism, and critical quench conditions.

To unify derivations throughout the text, the following physical symbols are fixed:

e denotes elementary charge, ε_0 vacuum permittivity, μ_0 vacuum permeability;

μ represents the equivalent magnetic dipole moment of electron standing waves, a lattice constant (average spacing between adjacent electrons);

k_B 为 Boltzmann constant, T thermodynamic temperature;

E external electric field strength, B external magnetic induction;

U_e electrostatic interaction potential between electrons, U_m magnetic dipole interaction potential.

3.1 Electromagnetic Competition Between Adjacent 8-Character Magnetic Moments

The conduction electrons in metals can be equivalently modeled as single clusters with fixed charges and intrinsic magnetic dipole moments, referred to as **8-shaped magnetic moments**. Between adjacent **8-shaped magnetic moments**, there exist both electrostatic repulsion and magnetic dipole attraction. The competitive relationship between these two potential energies forms the fundamental basis for the stable formation of magnetic coupling units and electron magnetic chains.

In the absence of external fields and under high-temperature conditions, the intrinsic drift of **8-shaped magnetic moments** leads to a random distribution of magnetic moment orientations, resulting in a statistically averaged net magnetic moment of zero for the system:

$$< \mu >_T = 0 \qquad (1)$$

. At this point, the magnetic dipole interactions between all electrons cancel each other out, leaving only the Coulomb electrostatic repulsion generated by like charges. If the average spacing between two adjacent **8-shaped magnetic moments** is the lattice constant a, the electrostatic repulsion potential energy is given by:

$$U_e(a) = \frac{e^2}{4\pi\varepsilon_0 a} \qquad (2)$$

$U_e(a) > 0$, manifesting as a repulsive interaction.

This naturally hinders electrons from approaching and pairing. Under high-temperature conditions, the thermal lattice disturbance energy far exceeds the weak transient magnetic coupling energy:

$$k_B T \gg |U_m| \qquad (3)$$

8-shaped magnetic moments cannot form stable, ordered coupling, and electrons remain in a mutually repulsive, discrete transport state. Consequently, the material exhibits conventional conductive properties with inherent electrical resistance.

When the system enters low-temperature conditions, lattice thermal motion is significantly suppressed, and electron thermal kinetic energy is greatly reduced, satisfying:

$$k_B T \ll |U_m| \qquad (4)$$

Under the action of an external magnetic field, the **8-shaped magnetic moment** is constrained by orientation potential energy:

$$U_B = -\boldsymbol{\mu} \cdot \boldsymbol{B} = -\mu B \cos\theta \qquad (5)$$

where θ is the angle between the **8-shaped magnetic moment** and the external magnetic field. The system spontaneously tends to the lowest energy state, with all **8-shaped magnetic moments** preferentially aligned along the external field, leading to spontaneous symmetry breaking in spatial symmetry. The magnetic moments transition from a disordered state to a long-range ordered state, and the global statistical average magnetic moment no longer remains zero:

$$< \mu > \neq 0 \qquad (6)$$

The magnetic moments transition from a disordered state to a long-range ordered state, and magnetic dipole interactions formally dominate the system's behavior.

Core criterion for superconducting phase transition: magnetic dipole attraction **overcomes electrostatic repulsion**

After magnetic order is established, adjacent electrons' **8-shaped magnetic moments** form stable heteropolar coupling, generating sustained magnetic dipole attraction potential energy:

$$U_m(a) = \frac{\mu_0}{4\pi} \cdot \frac{\boldsymbol{\mu_1 \cdot \mu_2}}{a^3} \qquad (7)$$

$U_m(a) < 0$, manifesting as mutual attraction.

In the formula $U_m(a) < 0$, it represents the typical attractive potential energy, which has the physical tendency to counteract electrostatic repulsion, bring closer the **8-shaped magnetic moments**, and promote the formation of magnetic coupling units. Consequently, the system forms a core potential energy competition pattern of "electrostatic repulsion hindering pairing, **8-shaped magnetic moments** attraction promoting pairing."

Temperature directly regulates the intrinsic drift kinetic energy of the **8-shaped magnetic moments**: in low-temperature environments, thermal excitation weakens, the overall drift amplitude of the **8-shaped magnetic moments** is compressed, the average electron spacing decreases, the asymmetric localized electromagnetic fields within each electron fully overlap, and the magnetic dipole attraction dominates, satisfying the energy criterion to spontaneously form stable magnetic coupling units. When the temperature rises, the intrinsic drift kinetic energy increases synchronously, electrons disperse from each other, the localized coupling between **8-shaped magnetic moments** significantly attenuates, the magnetic binding energy becomes insufficient to resist thermal disturbances, the magnetic coupling units dissociate, the **electron magnetic chains** break, and superconducting properties vanish.

3.2 Zero-Coupling Window Pairing Stability Modulation Mechanism

Electron **8-shaped magnetic moment** exhibits triaxial intrinsic drift periodic motion, with the magnetic axis periodically flipping and the magnetic moment direction alternating. At the instant of magnetic moment polarity switching, the internal dual-loop magnetic fields cancel each other, resulting in a transient zero-coupling window where the equivalent magnetic moment of the unit resets to zero. Within this window, the magnetic dipole attraction between adjacent **8-shaped magnetic moments** vanishes, leaving only electrostatic repulsion, which affects the average magnetic coupling and pairing stability.

The oscillation frequency of the 8-shaped magnetic moment is extremely high, and the zero-coupling window duration is exceedingly short. For the majority of the cycle, adjacent **8-shaped magnetic moments** are reverse-complementary, with magnetic dipole attraction potential exceeding electrostatic repulsion, ensuring the overall coupling network remains intact.

At low temperatures, all **8-shaped magnetic moments** are phase-synchronized, causing zero-coupling windows to occur simultaneously. As the temperature approaches T_c, thermal disturbances disrupt phase coherence, leading to staggered zero-coupling windows among individual **8-shaped magnetic moments**, thereby maintaining effective magnetic coupling locally throughout the system.

Let the full oscillation period of intrinsic drift be T_d, and the zero-coupling duration within a single cycle, where magnetic moment reversal cancellation and magnetic coupling failure occur, be Δt_0. The effective magnetic coupling duty ratio η is defined as:

$$\eta = \frac{T_d - \Delta t_0}{T_d} \quad , \ 0 < \eta < 1$$

The duty cycle $\boldsymbol{\eta}$ represents the proportion of time during a complete drift cycle that the system experiences effective magnetic dipole attraction coupling. Since within the zero-coupling window $\boldsymbol{U_m = 0}$, the true effective average magnetic dipole attraction potential

energy of the system requires correction by the duty cycle:

$$\overline{U_m}(a) = -\eta \cdot \frac{\mu_0}{4\pi} \cdot \frac{|\boldsymbol{\mu_1} \cdot \boldsymbol{\mu_2}|}{a^3} \quad (8)$$

. Temperature and external fields can directly modulate the width of the zero-coupling window: increasing temperature intensifies thermal disturbances, disrupting the **8-shaped magnetic moment**'s intrinsic drift regularity, prolonging the zero-coupling ineffective duration, reducing the duty cycle η, and significantly weakening the average magnetic dipole attraction strength. Under low-temperature order and external field orientation stabilization conditions, the zero-coupling window is compressed, η approaching 1, maximizing magnetic coupling efficiency and markedly enhancing the stability of the paired system.

This modulation mechanism explains the temperature sensitivity of the superconducting state: the zero-coupling window is an inherent microscopic instability channel of the system, determining that the magnetic dipole attraction cannot be infinitely strengthened, and there objectively exists critical stability conditions, providing a microdynamic basis for subsequent derivations of critical temperature and critical magnetic field.

3.3 Magnetic Coupling Single-Unit Energy Criterion $|U_m| > U_e$ Derivation

By combining the electrostatic repulsion potential energy with the average magnetic dipole attraction potential energy corrected by the zero-coupling window, the necessary and sufficient conditions for the spontaneous stable formation of magnetic coupling units can be strictly derived: the absolute value of the magnetic dipole attraction potential energy must be greater than the electrostatic repulsion potential energy, ensuring that the total interaction energy of the two-electron system is negative, thereby forming a bound steady state.

$$|\overline{U_m}(a)| > U_e(a) \quad (9)$$

Substituting Equations (2) and (8) into the criterion, we obtain:

$$\eta \cdot \frac{\mu_0 \varepsilon_0 |\boldsymbol{\mu_1} \cdot \boldsymbol{\mu_2}|}{a^2} > e^2 \quad (10)$$

This equation serves as the core theoretical criterion for the formation of magnetic coupling units in this study. From Equation (10), it can be seen that a decrease in the lattice constant a (high-pressure lattice compression), an increase in the effective magnetic moment of electrons, and an enhancement of intrinsic drift order (η approaching 1) can effectively satisfy the pairing conditions and improve superconducting stability, which is fully consistent with the experimental observation that high pressure increases the critical temperature of superconductivity.

Under the low-temperature ordered state that satisfies the above energy criterion, all **figure-8 magnetic moments** in the system achieve global phase locking:

$$\phi_i = \phi_j = \phi_0 (\forall i, j) \quad (11)$$

$(\forall i, j)$: A mathematical logic symbol, read as "for all i、j"; in the equation,

represents the phase of any two ϕ_i、ϕ_j figure-8 magnetic moments**.**

Any **8-shaped magnetic moment** phases are fully synchronized, and the coupled network forms a coherent system that can translate uniformly as a whole to generate macroscopic superconducting current. The current density satisfies:

$$\boldsymbol{J} = -\boldsymbol{nev} \quad (12)$$

$\boldsymbol{J}$ is the current density vector, describing the magnitude and direction of current per unit cross-sectional area, unit: A/m^2.

n is the carrier number density, e electron charge, and v_d is the overall drift velocity of the network.

8-shaped magnetic moment topological structure, magnetic moment arrangement, and phase remain stable at all times. Lattice vibrations and defects cannot cause scattering, resulting in zero system resistance term:

$$F_{scat} = 0 \qquad (13)$$

This manifests macroscopically as the zero-resistance effect.

Mathematical description of the Meissner effect

The ordered magnetic moment network induces a reverse magnetization intensity M, and the total magnetic induction intensity inside the superconducting material is:

$$B_{in} = B_{ext} + \mu_0 M \qquad (14)$$

Under complete diamagnetic conditions, the internal magnetic field is zero $B_{in} = 0$, leading to:

$$M = -\frac{1}{\mu_0} B_{ext} \qquad (15)$$

The induced magnetization completely cancels out the external field, achieving the Meissner perfect diamagnetic effect.

$\boldsymbol{M}$：Magnetization, the vector sum of the **8-shaped magnetic moments** per unit volume;

Critical parameters and quench conditions

Critical temperature $\boldsymbol{T_c}$

Based on the net coupling energy, the superconducting critical temperature $\boldsymbol{T_c}$ can be defined: The critical condition where thermal energy exactly cancels the net binding energy of the pairs is:

$$k_B T_c = |\overline{U_m}(a)| - U_e(a) \qquad (16)$$

$T < T_c$ When magnetic coupling dominates, Cooper pairs stably exist;

$T > T_c$ When thermal motion disrupts the pairing network, magnetic coupling units destabilize and vanish.

The critical magnetic field is determined by the external field's destruction condition of the magnetic moment ordered structure:

The external magnetic field applies an orientational torque on the 8-shaped magnetic moments. When the external field's potential energy is sufficient to counteract the system's average magnetic coupling binding energy and disrupt the ordered arrangement of magnetic moments, the system reaches the critical magnetic field:

$$\mu B_c \geq |\overline{U_m}(a)| \qquad (17)$$

$B > B_c$ At this point, the long-range order of the **8-shaped magnetic moments** disappears. The magnetic dipole attraction potential energy becomes insufficient to counterbalance the electrostatic repulsion, leading to the dissociation of magnetic coupling units and conventional quenching. If the magnetic field is further increased to an extremely high level, the external field can forcibly realign all magnetic moments in the same direction again, restoring magnetic coupling, corresponding to the experimentally observed high-field reentrant superconductivity phenomenon.

The critical electric field $\boldsymbol{E_c}$ and the critical magnetic field $\boldsymbol{B_c}$ are the two fundamental quench boundary conditions of the system.

The critical electric field is constrained by the stability of the intrinsic topological structure of the **8-shaped magnetic moment**: the external electric field accumulates potential energy over the spatial scale of the **8-shaped magnetic moment**. When the work done by the electric field is sufficient to counteract the self-sustaining binding energy of the **8-shaped magnetic moment**, the closed-loop 8-shaped structure will be torn apart. The critical criterion is given by:

$$eE_c \cdot L \geq E_{wave} \qquad (18)$$

L represents the spatial scale of the standing wave, E_{wave} is the intrinsic binding energy of the 8-shaped magnetic moment; an electric field exceeding the critical value E_c will directly disrupt the fundamental topology of the **8-shaped magnetic moment**, leading to the complete disintegration of the superconducting state.

4.0 Long-Range Magnetic Coupling — Quantum Anomaly Analysis Based on 8-Shaped Magnetic Moments

4.1 Superconducting Anomalous Behavior — Coupling Mechanism of 8-Shaped Magnetic Moments

High-pressure phononless superconductivity, magnetic field window-induced superconductivity, moiré superlattice twist angle T_c periodic oscillations, low-temperature metal parallel weak-field conductance single-peak anomaly, cross-dimensional quantum Hall states, two-dimensional van der Waals system magnetoelectric reversible regulation, cobalt-based triangular lattice spin supersolid dissipationless long-range spin order, aperiodic lattice ideal amorphous long-range magnetic coherence, pseudogap pre-pairing precursor phase, high-frequency microwave pairing relaxation loss, and other cross-material, cross-dimensional, multi-type cutting-edge experimental observations cannot be coherently explained by existing theories such as BCS phonon pairing, classical Lorentz magnetoresistance, or conventional spin pairing. All these disparate quantum behaviors share a unified underlying physical cause— **8-shaped magnetic moments** mediating interlayer long-range magnetic coupling. This chapter selects four representative cases for comprehensive deduction, while identifying three common core theoretical gaps that traditional theories fail to address, fully demonstrating the universal explanatory capability of this coupling mechanism.

4.2 Blue Light Periodic Depression—8-Shaped Magnetic Moment Collective Standing Wave Resonance

The traditional BCS superconductivity theory, based on electron-phonon coupling for pairing[2], predicts only broad, continuous phonon absorption spectra in optical absorption, lacking periodic discrete transmission depressions, and thus cannot explain the equally spaced regular periodic spectral attenuation signals observed in the blue light band.

Based on the **8-shaped magnetic moment** topological magnetic dipole model: In the low-temperature superconducting state, the **8-shaped magnetic moments** within all electronic magnetic maintain global phase coherence. A large number of electrons form synchronized self-sustained oscillations, constructing a collective electromagnetic resonance system with discrete

eigenenergy levels. When the incident blue photon energy matches the collective oscillation energy levels of the **8-shaped magnetic moments**, the photon energy is resonantly absorbed by the coherent electron clusters, resulting in periodic equidistant dips in the transmission spectrum. Upon increasing the temperature to the normal state, the long-range coherence of electronic magnetic chains collapses, the collective resonance effect vanishes, and the periodic spectral dips completely disappear.

The periodicity of spectral dips is uniquely determined by the intrinsic oscillation spatial scale of the **8-shaped magnetic moments**; the dip depth is positively correlated with the ordered electronic magnetic chain number density. When the external magnetic field is gradually increased to the critical field, the interlayer ordered arrangement of **8-shaped magnetic moments** is disrupted, leading to a continuous attenuation of dip depth until complete disappearance.

4.3 High-Frequency AC Loss — Dissociation Mechanism of 8-Shaped Magnetic Moment Chains

Under the traditional BCS theory framework, alternating electromagnetic fields only act on the lattice phonon system. AC losses solely originate from quasiparticle scattering caused by lattice defects and impurities, with no dissipation channels arising from dynamic regulation of electronic magnetic dipoles. This framework fails to explain the experimental observation that superconducting high-frequency AC losses increase with both the frequency and strength of the alternating field.

Under DC steady-state conditions, electrons drift uniformly and directionally, generating a constant circular self-generated magnetic field. All figure-8 magnetic moments are stably constrained in their orientations, and the interlayer magnetic coupling maintains a complete long-range electron magnetic linkage, with an extremely low probability of magnetic linkage dissociation, which macroscopically manifests as zero resistance.

When high-frequency alternating current is applied, the periodic rapid reversal of current direction directly causes changes in the strength and direction of the self-generated magnetic field, severely affecting the generation of figure-8 magnetic moments. Simultaneously, this directly leads to an increased probability of electron magnetic linkage dissolution and zero-crossing dissociation.

The higher the current reversal rate (i.e., greater alternating frequency f) and the larger the AC current amplitude I_{ac}, the steeper the field gradient during single magnetic moment reversal becomes. This prolongs the duration of the dissociation window corresponding to magnetic moment zero-crossing, significantly increasing the total proportion of paired dissociations within a single alternating cycle. The concentration of dissociated single-electron charge carriers within the system concurrently rises. The dissociated free electrons lose long-range coherent transport constraints, undergo momentum scattering, and release thermal energy, resulting in a macroscopic equivalent high-frequency AC resistance that increases with both alternating frequency and current amplitude.

4.4 Non-monotonic Low-Temperature Weak-Field Conductivity – Figure-8 Magnetic Moment Regulation Mechanism

Observations in numerous pure elemental metals (conventional superconducting metals like Al, Pb, Sn) at low temperatures reveal:

Applying a weak static magnetic field parallel to the current direction → the resistance first slightly decreases (conductivity improves); after the magnetic field exceeds a critical value, the resistance instead continues to rise, exhibiting a "conductivity first rises then falls" single-peak curve.

Limitations of existing theories: Classical Lorentz magnetoresistance can only explain that the higher the magnetic field, the higher the resistance, and is completely unable to account for the behavior of resistance reduction in the weak field interval, which belongs to a recognized theoretical gap.

Peking University in 2026 discovered in rhombohedral multilayer graphene: the zero magnetic field is an insulating state, and applying a specific in-plane weak magnetic field directly transitions it to a superconducting state; magnetic fields that are too low or too high will exit superconductivity, with only a magnetic field window existing for stable superconductivity.

Anomalous points: Traditional theories suggest that magnetic fields only destroy spin pairing and suppress superconductivity, but this system demonstrates that a weak magnetic field with suitable orientation can instead induce electron pairing and open superconducting channels. Current mainstream theories can only qualitatively describe this and struggle to fully explain the microscopic mechanisms.

Magnetic field-induced superconducting phase diagram

5.0 Superconducting conductor DC self-field layered observation experiment

5.1 Experimental microscopic mechanisms and theoretical foundations

Under constant DC conditions, superconducting conductors generate a surrounding self-induced magnetic field. In the classical uniform current-carrying model, the current density is equal everywhere. According to Ampère's circuital law, the internal magnetic field of the conductor satisfies $B(r) \propto r$, with the magnetic field increasing linearly with radial distance. Under the electron magnetic chain model, the self-generated magnetic field causes electrons to form an 8-shaped magnetic moment. Adjacent magnetic moments couple with opposite poles, arranging circumferentially to form a ring-shaped electron magnetic chain. The stronger the magnetic field, the higher the order of the magnetic chain, causing current to concentrate towards the surface, with current density increasing radially outward.

This current distribution leads to the conclusion that the internal magnetic field satisfies $B(r) \propto r^2$, and the magnetic field grows quadratically with radial distance.

Existing classical superconductivity theories can only qualitatively describe flux pinning and fail to quantitatively explain the radial current stratification phenomenon in superconducting cylinders under DC conditions. This experiment aims to verify this discrepancy.

5.2 Derivation of Magnetic Field Distribution Formula and Experimental Predictions

Relationship between current and zero resistance in superconducting conductors: Within the linear range of the self-generated magnetic field, as the total current increases, the self-generated magnetic field continuously strengthens, magnetic chain order improves, and the conductor's equivalent loss gradually decreases. In a certain range, conduction resistance is positively correlated with total current. After reaching a specific current value, the conductor maintains near-zero resistance.

Superconducting conductors exhibit skin effect under DC conditions: Influenced by the radial magnetic field gradient, superconducting cylinders under DC steady-state conditions show distinct radial current stratification, forming a DC skin distribution. According to model derivation, when conducting DC current, the magnetic field intensity at different radial positions in the superconductor satisfies the relationship: $\frac{B_2}{B_1}=\frac{R_2^2}{R_1^2}$,$\frac{B_3}{B_1}=\frac{R_3^2}{R_1^2}$. Below is the derivation of this relationship.

Sample Geometry: The sample is a single-crystal superconducting solid cylinder with radius $R3$. The outer measurement hole bottom is located at radii $R1$、$R2$, from the axis:

$$R_1 = 5\ mm\ , R_2 = 7.07\ mm\ , R_3 = 10\ mm$$

A constant direct current I is applied; the axis center is $r = 0$, and the outer wall is $r = R$.

Current Distribution Assumption: It is assumed that the internal current density increases linearly along the radial direction:

$J(r) = Ar$

A are constants, with higher current density closer to the outer wall.

Theoretical Derivation:

- **The current enclosed within radius r is**

$$I_{enc}(r) = \int_0^r Ar' \cdot 2\pi r' dr' = \frac{2\pi A}{3} r^3$$

1. . Internal magnetic field (using Ampère's circuital law):

$$B(r) = \frac{\mu_0 I_{enc}(r)}{2\pi r} = \frac{\mu_0 A}{3} r^2$$

.The internal magnetic field is proportional to the square of the radial coordinate: $B(r) \propto r^2$.

- **Outer Wall Boundary Verification:**

Let $r = R$ to obtain the total current $I = \frac{2\pi A}{3} R^3$. Substituting into the outer wall magnetic field:

$$B(R) = \frac{\mu_0 I}{2\pi R}$$

,which matches the standard formula for the external magnetic field of a long straight cylinder, confirming model self-consistency.

- **Theoretical Ratio Prediction:**

$$\frac{B_2}{B_1} = \frac{R_2^2}{R_1^2} = 2 \quad \frac{B_3}{B_1} = \frac{R_3^2}{R_1^2} = 4$$

By measuring the relative ratio of the magnetic field at three internal positions of the conductor, the inverse square relationship can be verified, thereby validating the electron magnetic chain

model of DC skin layering.

5.3 Experimental Setup and Procedure

Cryogenic vacuum variable-temperature sample stage, non-contact nanoscale scanning Hall probe system, high-precision low-ripple DC current source, multi-channel weak signal acquisition host.

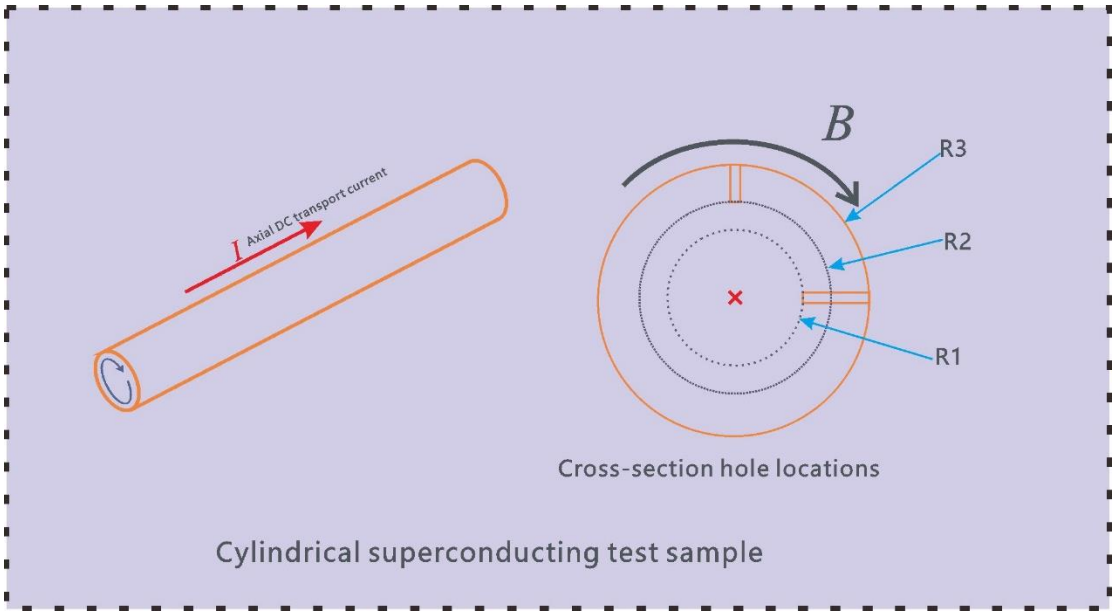

Figure 5 Cylindrical superconducting specimen. Holes at radii R_1, R_2, R_3 measure circumferential magnetic field to verify$B \propto r^2$.

The specimen is a single-crystal superconducting solid cylinder without grain boundaries, with an outer diameter of 20 mm, and polished overall. Micro-holes are drilled radially along the sidewall of the cylinder, with the hole bottom radii from the axis being $r = 5\,mm$、$r = 7.07\,mm$. The hole diameter is kept as small as possible while allowing the probe to enter the interior of the specimen, enabling fixed-point measurement of the internal magnetic field and avoiding data bias caused by surface measurements.

1) Fix the superconducting cylindrical specimen on the cryogenic vacuum sample stage, evacuate to high vacuum, and cool below the superconducting transition temperature. Use the four-probe method to calibrate the zero-resistance interval of the specimen and determine the DC critical current I_C.

2) Set multiple constant DC currents, all current values are less than the critical current to prevent magnetic saturation and ensure the magnetic chain remains within the linear response range.

3) Insert the miniature Hall probe sequentially into the two radial microholes to measure the internal tangential magnetic field at $r = 5\,mm$、$r = 7.07\,mm$、$r = 10\,mm$ three positions, and record the magnetic field data for each group.

4) Calculate the magnetic field ratios at the three measurement points, compare them with the theoretical predicted values of $B(r) \propto r^2$, and analyze measurement errors to verify the DC skin layering effect.

5) Repeat the measurements under multiple current groups multiple times to eliminate

systematic and random errors caused by probe positioning and current fluctuations, obtaining stable and reliable experimental patterns.

5.4 Result Evaluation and Experimental Feasibility

Result Evaluation:

Use a low-temperature Hall probe to scan the cross-sectional magnetic field and invert the radial current density;

if the measured ratio is close to $\frac{B_2}{B_1} = 2$, $\frac{B_3}{B_1} = 4$, it proves that the hypothesis of a linear radial increase in current density within the superconductor holds; if the measured ratio significantly deviates from the theoretical value, it indicates that the internal current distribution does not satisfy the $J(r) \propto r$ linear distribution, requiring modification of the original current-carrying model.

Supplementary Prediction: In the DC variable current test, as the total loop current gradually increases, the self-generated magnetic field of the conductor synchronously strengthens, and the degree of ordered arrangement of electron magnetic chain continues to improve. Before reaching the critical current, the residual loss of the sample will gradually decrease as the current rises; when the current exceeds this linear range, the magnetic chain structure stabilizes, and the conductor resistance will remain stable at a level approaching zero. This variation pattern can serve as auxiliary observational evidence, corroborating the radial magnetic field distribution results.

Feasibility Explanation:

Most existing published literature only conducts magnetic field testing on the surface of superconducting conductors, with very few performing fixed-point measurements of the internal radial magnetic field. This experiment employs a single-crystal, grain-free, solid superconducting cylinder, using radial position as the sole variable to avoid interference from grain boundaries and structural defects. A quantitative correspondence is established between the self-generated magnetic field, the orderliness of electron magnetic chain, and the current-carrying stratification effect under pure DC conditions.

The testing equipment used in this experiment consists of mature commercial instruments, with single controllable variables and self-consistent logic, enabling direct verification of the proposed figure-8 magnetic moment and electron magnetic chain micro-transport mechanisms in this paper. The research plan demonstrates strong feasibility and academic originality.

6.0 Model Innovations and Research Value

6.1 8-Character Magnetic MomentModel vs. Traditional BCS Model

Table

Comparison Dimensions	Traditional BCS Superconducting Model	8-Character Magnetic Moment Topological Model
Electron Interaction Mode	Only allows localized pairwise coupling to form Cooper electron pairs	Forms global topological coupling, constructing a continuous standing wave network

Coupling Mechanism	Relies on lattice phonons for indirect coupling	Relies on electron standing wave fields for direct magnetic topological coupling
Thermal Disturbance Stability	Structure is highly susceptible to thermal disturbances, with rapid pair dissociation at high temperatures	Ordered structure exhibits stronger resistance to thermal disturbances
Charge Transport Mechanism	Relies on collective Bose condensation of Cooper pairs for directional drift	Relies on synchronized translation of the entire standing wave network for conduction
External Field Response Characteristics	Can only qualitatively explain magnetic field suppression of superconductivity	Can provide microscopic mechanisms for multi-field regulation behaviors under electric fields, magnetic fields, and pressure

6.2 Unified Explanatory Capability for Various Anomalous Superconducting Phenomena

- **Changes in the Pairing Structure**

The BCS theory strictly limits electrons to pair only in pairs, with a fixed binary unit structure. In the chain magnetic coupling model, the number of paired units is no longer restricted. The **8-shaped magnetic moments** connect end-to-end, forming a multi-electron continuous chain structure, breaking through the constraints of fixed two-electron pairing.

- **Simplification of the Interaction Mechanism**

The BCS theory must introduce lattice phonons as a medium to achieve electron attraction, making the theoretical framework more convoluted. This model relies on the intrinsic magnetic moments of electrons themselves to achieve magnetic dipole coupling, eliminating the dependence on lattice vibrations as an intermediate medium. The entire physical logic becomes more concise and self-consistent.

- **Updated Microscopic Mechanism of AC Loss**

The BCS theory can only vaguely describe energy loss caused by the repeated splitting and recombination of Cooper pairs under alternating current, failing to precisely localize the loss regions. The chain magnetic structure contains weakly coupled segments. When the alternating current crosses zero, local chain breaks occur, and the structure automatically reorganizes after the field strength recovers. This allows for a quantitative description of the periodic dissociation process, aligning with experimental observations of AC superconducting losses.

- **Expansion of Applicable System Scope**

The BCS theory is only applicable to conventional low-temperature metallic superconductors and struggles to explain unconventional systems such as copper-based high-temperature superconductors [3] and magic-angle graphene flat-band superconductivity. The chain magnetic coupling structure better aligns with two-dimensional, strongly correlated superconducting systems dominated by magnetic interactions, offering broader applicability.

- **Microscopic Current-Carrying Image Correction**

Under the BCS framework, Cooper pair electron clouds are arranged in a widely dispersed manner. In the magnetic chain model, electrons are magnetically coupled and constrained to fixed orbits for ordered motion, with disordered scattering significantly suppressed, eliminating

the need for additional complex momentum cancellation assumptions to explain zero resistance.

- **Optimization of Many-Body Collective Behavior Description**

BCS treats a large number of independent electron pairs as isolated quantum condensation units, with weak long-range correlations between electrons. The electron magnetic chain belongs to a continuous, integrated ordered structure, where adjacent units exhibit long-range coupling and联动, better aligning with the collective experimental characteristics of strongly correlated superconducting systems.

6.3 Research Value of the Magnetic Coupling Pairing Model

Existing conventional superconducting theories have long been confined to the framework of two-electron pairing and phonon coupling, struggling to provide self-consistent microscopic explanations for numerous unconventional superconducting experimental phenomena. Starting from the **8-shaped electromagnetic standing wave + intrinsic drift electron structure**, this model establishes a chain-like ordered arrangement mechanism. It not only explains the radial current stratification phenomenon in superconducting conductors under direct current but also offers coherent physical interpretations for alternating current loss, magnetic field调控, flat-band system superconductivity, and other experimental observations. The entire derivation is grounded in electromagnetic coupling and topological structures, requiring fewer mathematical assumptions and providing more intuitive physical imagery, thereby offering a new analytical approach for subsequent research on superconducting microscopic mechanisms.

7.0 Conclusions and Prospects

Based on the **8-shaped electromagnetic standing wave + intrinsic drift electron structure**, this paper establishes a complete derivation process extending from the microscopic intrinsic electronic structure to macroscopic superconducting transport effects. This model no longer relies on phenomenological assumptions such as phonon interactions or Cooper pairing, constructing a logically self-consistent, physically concise, and observationally predictive microscopic mechanism.

This paper proposes that the mechanism of superconductivity does not rely on electron-phonon interactions condensing into Cooper pairs. Under the combined effects of an external electric field, self-generated magnetic fields, and low-temperature conditions, the **8-shaped magnetic moments** of electrons form ordered arrangements, coherently condensing into **electron magnetic chain** arrays. Within the system, magnetic dipole interactions dominate, suppressing electrostatic repulsion between electrons, thereby achieving dissipationless directional transport of carriers.

This model can provide reasonable microscopic physical explanations for conventional low-temperature superconductivity, high-temperature superconductivity[3], pressure-regulated superconductivity, and transport behavior under magnetic fields. It also offers experimentally observable predictions for carrier distributions, providing new analytical approaches for subsequent research on superconducting mechanisms.

The authors declare that no financial support was received for this research.

References

[1] Z. L. Sun. 8-shaped Electromagnetic Standing Wave + Eigen Drift Electron Structure[EB/OL]. Zenodo, 2026. doi 10.5281/zenodo.20626931.
[2] Bardeen J, Cooper L N, Schrieffer J R. Theory of Superconductivity[J]. Physical Review, 1957, 108(5): 1175-1204.
[3] Zhao Z X. Research progress of high-temperature superconducting materials and physics[J]. Acta Physica Sinica, 2018, 67(20): 207401.